Journal of Materials Chemistry A

Accepted Manuscript

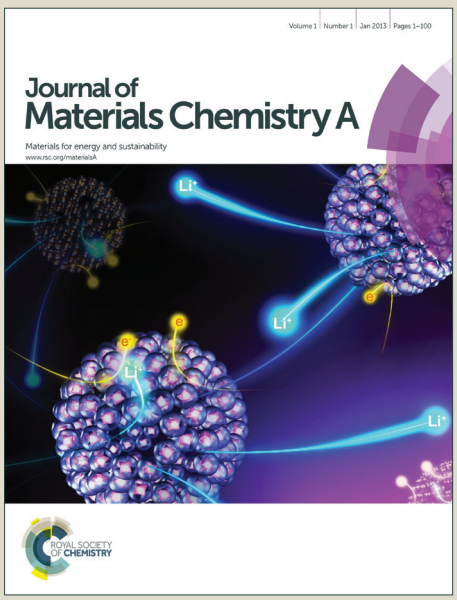

ROYAL SOCIETY OF CHEMISTRY

www.rsc.org/materialsA

Journal Name

RSCPublishing

ARTICLE

High-performance Hg^{2+} removal from ultra-low-concentration aqueous solution using both acylamide- and hydroxyl-functionalized metal-organic framework

Cite this: DOI: 10.1039/xoxxoooooox

Received ooth January 2012,
Accepted ooth January 2012

DOI: 10.1039/xoxxoooooox

www.rsc.org/

Feng Luo,* Jing Li Cheng, Li Long Dang, Wei Na Zhou, Hai Lv Lin, Jiang Qiang Li, Shu Juan Liu, and Ming Biao Luo

Mercury (Hg^{2+}), even ultra-low-concentration amount in water, presents a serious environment concern. Thus, the removal, especially Hg (II) content in the ultratrace level (ppb), from water is still challenging. In this work, without any pretreatment, one novel MOF material can act as high-capacity and collectable adsorbent for the removal of Hg (II) from water, especially for ultratrace Hg^{2+} ion in the ppb magnitude, mainly due to a combined effect from the pore walls functionalized by free-standing, accessible acylamide and hydroxyl units.

Introduction

Mercury, a highly toxic and bio-accumulative heavy metal, shows strong biological toxicities to people's health[1]. The main chemical species of mercury are element mercury (Hg^0), inorganic mercury (Hg^{2+}) and methylmercury (MeHg). In particular, divalent mercury (Hg^{2+}) is a wide-spread environment pollutant, and mainly found in surface water. It is reported that contaminated natural waters usually contain Hg in the magnitude of ppb level.[2] However the fact proved that Hg^{2+} poses human risks even at relatively low dosages.[3,4] The World Health Organization (WHO) has set the maximum level of mercury contamination in drinking water at 1 ppb.[5] However, the mercury removal efficiency by means of traditional mercury removal technologies is still not satisfied, such as ion exchange, amalgamation, chemical precipitation, and membrane separation,[6,7] because of invalidation of the materials used when facing ultra-low-concentration Hg^{2+} system. As a consequence, developing more efficient Hg^{2+} removal material, especially aiming at ultra-low-concentration Hg^{2+} system, is very important for water safety.

Metal–organic frameworks (MOFs) are inorganic-organic solids that form porous crystalline structures and can be synthesized by using a wide range of metal ions and organic ligand.[8] MOFs are of great interest for technical applications such as gas adsorption separation,[9] catalysis,[10] drug delivery[11] and sensing due to their unique properties. Their crystalline nature, high porosities, extraordinary surface areas, finely tunable pore surface properties, and potential scalability to industrial scale have made these materials as an attractive target for further study.[12] It has reported that adsorption is an efficient method to remove heavy metal from aqueous solutions. Recently, researchers start to evaluate MOFs as adsorbents in the aqueous environment.[13] A few MOFs also have been used in removal of heavy metal, such as mercury,[14,15] revealing that MOFs can be stable in water and exhibit great capacity to isolate the target contaminant. In this work, we describe a novel MOF material that shows excellent capability towards removal of ultratrace Hg^{2+} ion even in the magnitude of 1 ppb.

Results and discussion

The MOF adsorbent, Zn(hip)(L)·(DMF)(H_2O) (H_2hip=5-hydroxyisophthalic acid, L=N^4,$N^{4'}$-di(pyridine-4-yl)biphenyl-4,4'-dicarboxamide) was prepared by solvo(hydro)thermal syntheses strategy.[16] Typically, DMF/H_2O (6 mL,5:1) solution of $Zn(NO_3)_2$, L, H_2hip (5-hydroxyisophthalic acid) in a ratio of 1:1:1 was sealed in a Teflon reactor, and heated at 120℃ for 2 days, then cooled to the room temperature at 3℃/h. The phase purity is confirmed by XRD investigation (Fig. S1). The outstanding structure feature of it is the 1-D regular hexagonal channel along the *c* axis with effective aperture of ca. 5.4Å and abundant both acylamide and hydroxyl groups located on the pore wall (Fig. 1).

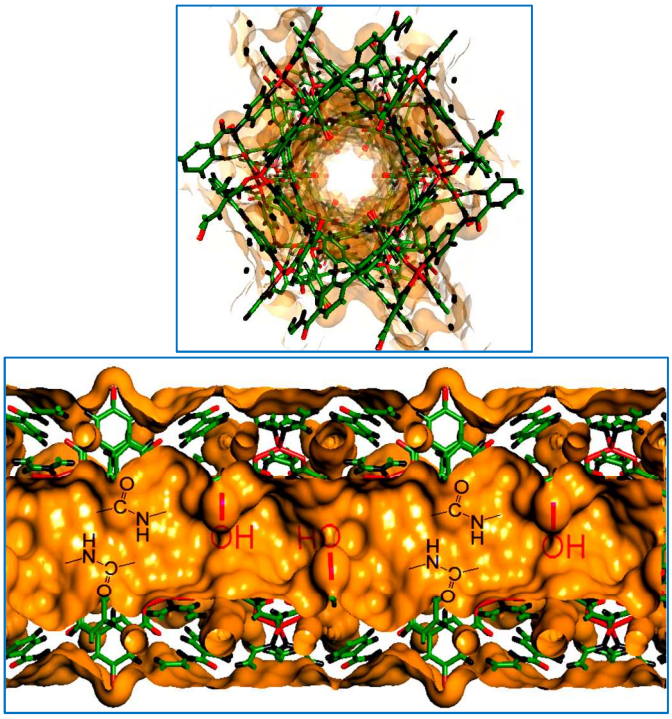

Fig. 1 Overlooking the 1D channel in the MOF along *c* axis and the section description of the both acylamide- and hydroxyl-functionalized 1D channel.

To demonstrate the effective mercury capture from water, a series of batch adsorption tests were conducted to examine the effects of pH, contact time, temperature, and initial concentration on Hg(II) uptake by the adsorbent. Stock solution of Hg(II) (1000 mg L^{-1}) was prepared from $Hg(NO_3)_2$. All the working Hg(II) solution were prepared using appropriate subsequent dilutions of the stock solution. The adsorption of Hg(II) was assessed under static condition. The pH of the Hg(II) solution was adjusted to required value by using a HCl and $NH_3 \cdot H_2O$ solution. The residual concentration of the Hg^{2+} in the solution was determined by atomic fluorescence spectrometer (AFS). The amount of adsorption at equilibrium, q_e (mg/g),was calculated according to Eq. (1):[17]

$$q_e = \frac{(c_0 - c_e)v}{m} \quad (1)$$

Where c_0 (mg L^{-1}) and c_e (mg L^{-1}) are the initial and equilibrated concentrations of Hg^{2+}, respectively, v (L) is the volume of solution, and m (g) is the mass of dry adsorbent. The removal efficiency (%) of the mercury was calculated by Eq. (2):

$$\text{Removal efficiency } (\%) = \frac{c_0 - c_e}{c_0} \times 100\% \quad (2)$$

One of the main factors that can modify the mercury adsorption efficiency is the solution pH, because multiple inorganic mercury species could be present in an aqueous solution depending on pH and chloride concentration. In order to illustrate the adsorption processes and mechanisms the effect of solution pH were studied. For an aqueous solution of mercury ions ($c_0 = 100$ppb), the effect of pH on the removal efficiency is showed in Fig. S2. It is illustrated that the removal efficiency was very low at strong acidic solution and increases with increasing pH values, until a certain pH value of 5 was reached, and then decreased at higher pH. This is because of the protonation effect on the surface of MOF adsorbent at low pH conditions, resulting in that the sorption of Hg^{2+} were restricted. Of course, other factors such as that the presence of excess H^+ ions offer competition between H^+ and Hg^{2+} for the sorption sites on the surface of adsorbent should be also accounted into. Accordingly, optimum pH value of 5 was selected for subsequent adsorption experiments.

In order to evaluate the kinetic mechanism that control the adsorption process, the effect of contact time on the adsorption of Hg(II) onto the MOF was investigated. 2 mg MOF adsorbent was added into 40 mL mercury ion solution ($c_0(Hg^{2+})$=100 ppb, pH=5), then shaken at 25℃ for a predetermined time. The effect of contact time at optimum pH and room temperatures is shown in Fig. S3. The results demonstrated that the adsorption was rapid within 30 minutes and then slowed considerably. It achieved equilibrium within 1 h. The adsorbent could remove 80% of Hg^{2+} ion from the solution within 1 h even when initial Hg^{2+} concentration was as low as 100ppb, suggesting that this MOF sorbent possesses high adsorption efficiency in the removal of Hg(II) from water.

Kinetic models are usually used to understand the mechanism of metal adsorption and the performance of the adsorbents for metal removal. The pseudo-first-order kinetic and pseudo-second-order kinetic model are the most typical ones. The pseudo-first-order model is expressed as

$$\ln(q_e - q_t) = \ln q_e - k_1 t \quad (3)$$

where q_e (mg g^{-1}) and q_t (mg g^{-1}) are the adsorption amounts at equilibrium and at time t, respectively, k_1 (min^{-1}) is the pseudo-first-order rate constant.

The pseudo-second-order model is expressed as

$$\frac{t}{q_t} = \frac{1}{k_2 q_e^2} + \frac{t}{q_e} \quad (4)$$

where k_2 (g (mg min^{-1})) is the pseudo-second-order rate constant. Fig. S3 shows the fitting result of experimental kinetic date for mercury adsorption on the MOF material by pseudo-first-order kinetic model and pseudo-second-order kinetic model.

The regression coefficient (R^2) and several parameters obtained from kinetic models are shown in Table 1.

Table 1 Kinetic parameters for adsorption of Hg^{2+}

	Pseudo-first-order kinetics			Pseudo-second-order kinetics		
$q_{e,exp}$	k_1	$q_{e,cal}$	R^2	k_2	$q_{e,cal}$	R^2
1.62	0.042	0.886		0.120	1.680	0.9992

As shown in Fig. S3 and Table 1, the pseudo-second-order model fits the data very well and provided better coefficients of determination than the pseudo-first-order for the adsorption of Hg(II) on adsorbent, suggesting that the pseudo-second-order model was more suitable for describing the current adsorption kinetic of Hg(II) ion. Furthermore, the calculated q_e value from

the pseudo-second-order model were in good agreement with the experimental value, $q_{e,exp}$. Thereby it is believed that both mechanisms of physisorption and chemisorption with different contribution should be involved in the current Hg(II) adsorption process. From the viewpoint of structure, both hydroxyl and acylamide groups in the pore wall hold the potential to coordinate with Hg(II) ions, thereby acting as strong sites for Hg(II) chemisorptions.

The adsorption capacity of the MOF adsorbent was investigated at pH 5 upon Hg^{2+} solution with concentration from 1 to 25 ppm. The uptake of Hg^{2+} by adsorbent can be described in the form of sorption isotherms, see Fig. 2. The existence of a plateau indicated the final saturation of MOF adsorbent, giving an unprecedented adsorption capacity of ca. 278 mg g^{-1} when initial Hg^{2+} concentration was 20mg L^{-1}. Such high capacity could be attributed to both hydroxyl and acylamide groups densely populated on the inner surface of porous MOF.

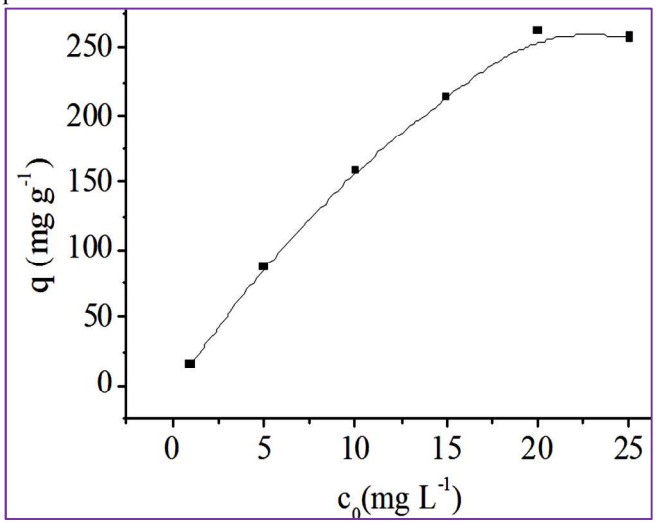

Fig. 2 Sorption isotherm of Hg^{2+} by the MOF material ($c_0(Hg^{2+})$=100 ppb,v=40 mL, m(adsorbent)=2 mg, T=25℃, t=1 h).

To analyze the equilibrium date, two common equilibrium models, the Langmuir adsorption isotherm and the Freundlich adsorption isotherm, were employed. The Langmuir model is monolayer sorption onto homogeneous surface.[18,19] In contrast, the Freundlich isotherm is applicable to both monolayer (chemisorptions) and multilayer adsorption (physisorption) and is based on the assumption that the adsorbate adsorbs onto the heterogeneous surface of an adsorbent.[20,21] The Langmuir isotherm is described as follows:

$$\frac{c_e}{q_e} = \frac{1}{q_{max}} K_L + \frac{c_e}{q_{max}} \quad (5)$$

The Freundlich is described as

$$\ln q_e = \ln K_F + \frac{1}{n} \ln c_e \quad (6)$$

Where q_e (mg g^{-1}) is the adsorption capacity, c_e (mg L^{-1}) is the equilibrium concentration of Hg^{2+}, K_L (mg L^{-1}) is the Langmuir adsorption constant, K_F (mg g^{-1}) and n are the Freundlich constants. The isotherm date fitted using Langmuir isotherm were represented by Fig. S4a and R^2 of the fitting line were shown in Table S1. The value of R^2 is 0.914. Subsequently, the adsorption isotherm date was analysed using Freundlich isotherm. The values of R^2 both the Langmuir and Freundlich models could be reasonable for describing the adsorption behaviour of Hg^{2+} onto the adsorbent. However, R^2 of the fitting (Fig. S4b, Table S1) by Freundlich model was not as high as that obtained by Langmuir isotherm, indicating that the Langmuir isotherm model more suitable for describing the adsorption isotherm of Hg^{2+} onto MOF material, implying that the surface of MOF is more homogeneous and dominating chemisorption mechanisms, very likely derived from Hg-O contacts from both hydroxyl and acylamide groups in the pore wall. The maximum adsorption capacity was calculated to be 333 mg g^{-1} by the Langmuir adsorption isotherm model, slightly bigger than the experimental value.

Thermodynamic analysis of mercury removal by adsorbent was assessed by energy change of adsorption. The thermodynamic parameters (enthalpy ΔH^0, entropy ΔS^0) of sorption of Hg^{2+} were determined by performing batch sorption experiments at 25℃, 35℃, 45℃. The energy change of adsorption was calculated by the following equation:

$$\Delta G = \Delta H - T \Delta S^0 \quad (7)$$

$$\ln Kd = \frac{\Delta S^0}{R} - \frac{\Delta H^0}{RT} \quad (8)$$

$$Kd = \frac{V}{m}\left(\frac{c_0}{c_e} - 1\right) \quad (9)$$

Where ΔG^0 (kJ mol^{-1}) is the Gibbs free energy change, ΔH^0(kJ mol^{-1}) is the change in enthalpy, ΔS^0 (J $(mol\ K)^{-1}$) is the change in entropy, Kd is the distribution coefficient of adsorption, R (8.314 J $(mol\ K)^{-1}$) is the universal gas constant, T (K) is Kelvin temperature. The values of ΔS^0, ΔH^0, and ΔG^0 are summarized in Table S2. The negative ΔH^0 values for the MOF adsorbents indicate that the adsorption process was exothermic. The positive values of ΔS^0 suggest that the randomness of the solid-solution interface increased during the Hg^{2+} sorption. The negative sign of ΔG^0 indicates that the adsorption of Hg^{2+} onto adsorbent was spontaneous.

Table 2 initial and final Hg^{2+} concentrations, removal efficiency

Initial Hg^{2+} concentration (ppb)	Final Hg^{2+} concentration (ppb)	Removal (%)
1.0	0.57	42.60
2.0	0.68	66.50
5.0	1.45	70.98
10.0	1.65	83.53
20.0	3.05	84.76

The qualitative study described above indicated that the MOF is excellent for the removal of Hg^{2+} ion from contaminated solutions. To demonstrate the effective Hg^{2+} capture from water, a MOF sample (2 mg) was added into a dilute aqueous solution (40 mL) of Hg^{2+} (pH=5). These solutions cover different concentrations of Hg^{2+} ranging from 1 to 20 ppb. The MOF sample is very effective in removing Hg^{2+} ion from solution with low initial concentration, see Table 2. After being stirred at room temperature for 1 hour, residual Hg^{2+} in solution become smaller than 1 ppb when the initial Hg^{2+} concentration as low as 2 ppb, lower than criterion of 1

ppb requested by the World Health Organization. And a 83.53% removal can be obtained when the initial Hg^{2+} concentration was 10 ppb. By contrast, the reported MOF material[22] shows outstanding and effective Hg^{2+} removal only in the 100 ppb magnitude of Hg^{2+} concentration and the residual is more than 10 ppb, much higher than the criterion of the World Health Organization. This strongly suggests that our MOF material is an excellent adsorbent towards Hg^{2+} removal, especially for ultra-low-concentration Hg^{2+} solution.

To confirm the chemic stability of the MOF material after loading Hg^{2+} ions, the powder X-ray diffraction (PXRD) investigation is employed. As shown in Fig. S5, the PXRD patterns of MOF material after loading Hg^{2+} ion match well with the as-synthesized samples, suggesting excellent chemic stability of it in this system. But, the lowest angle peak of 010 was greatly diminished. New peak appeared at $2\theta=7.7°$ and the peak of 012 shift towards high angle, as well as higher−angle peaks like that of 110, 013, 121, 131 became generally stronger. Such significant changes mainly reflect the large increase of electron density in the channel region, since the system becomes less porous as a result of the uptake of Hg(II) ions. Moreover, the filtrate was analyzed by IR and AFS, no obvious residue like that of organic ligand and Zn(II) ions, suggesting that part dissolution of MOF material in this system is excluded. Furthermore, the surface morphology and chemical composition of the MOF sample material after loading Hg^{2+} ions was characterized by SEM and EDX investigation (Fig. S6, 7). It is clear that the perfect hexagonal pillar-like crystals of as-synthesized samples are eroded after loading Hg^{2+} ions. The content shown by EXD spectra of Hg is 4.7 times bigger than Zn, approximately equal to adsorption amount of 360 mg/g, higher than the experimental and theoretical value, implying that the Hg^{2+} uptake is uneven for every MOF crystal and the experimental and theoretical value is an average statistical result. Moreover, the presence of Cl^- ions indicate the adsorption of $HgCl_2$ (exp. $HgCl_{1.7}$), where the Cl^- ions derived from HCl during adjusting pH value. Then, based on the max adsorption amount of Hg(II), element analysis (C 40.78%, H 2.65%, N 6.10%), as well as EXD result, we can deduce the chemical formula, $Zn(hip)(L)\cdot(H_2O)(HgCl_2)$, for the $HgCl_2$ loaded samples. To further confirm the loading of $HgCl_2$ in this MOF material, TG is investigated. In contrast to the as-synthesized samples that shows major weight loss (16%) of solvent molecule at 40-272°C, the $HgCl_2$ loaded samples at this region only gives a slight weight loss (2%, equal to one water molecule of 1.9%), directly supporting the fact of loaded $HgCl_2$. The difference of TG plots at 272-377°C between as-synthesized samples and $HgCl_2$ loaded samples indicates the loss of $HgCl_2$ (exp. 22%), small than the expected value of 28%, possibly due to the formation of HgO, as after 450°C the TG plots of them are also distinct (Fig. S8).

To relate the excellent adsorption performance and implied chemisorptions process with the MOF structure, IR spectrum is carried out for as-synthesized samples and $HgCl_2$ loaded samples. The characteristic O-H stretching bond at 2665 cm^{-1} becomes absent and new bond appears at 583 cm^{-1} in the $HgCl_2$ loaded samples, strongly suggesting the formation of Hg-O bond. Moreover, the great decrease in intensity of the characteristic C=O stretching bond at 1682 cm^{-1} for acylamide group also implies strong contact between $HgCl_2$ and C=O unit. Thereby, it is clear that the free hydroxyl and acylamide groups in the channel of MOF materials should be responsible for the present excellent adsorption performance.

Conclusions

This study systematically evaluates a novel MOF material with the pore wall functionalized by both hydroxyl and acylamide groups towards the removal of Hg^{2+} ions from water in detail. Notably, without any pre-treatment, this porous material shows a high affinity and significant adsorption capacity (278 mg g^{-1}) for Hg^{2+} removal from solution, thus preforming a big potential in Hg^{2+} removal from water. Importantly, for ultra-low-concentration Hg^{2+} aqueous solution ($c_0(Hg^{2+})$ <5 ppb), effective removal is also observed, such as an one-off removal efficiency of 66.5% can be obtained under a 2 ppb Hg^{2+} aqueous solution, below the criterion (1 ppb) of the World Health Organization. To some extent, this work has established a simple and efficient route to remove ultra-low-concentration Hg^{2+} ions from aqueous solution.

Acknowledgements

This work was supported by the NSF of China (21203022, 21261001, 21361001), the Natural Science Foundation of Jiangxi Province of China (no. 20143ACB20002), and the Young scientist training program of Jiangxi Province of China (no. 20142BCB23018).

Notes and references

College of Biology, Chemistry and Material Science, East China Institute of Technology, Fuzhou, Jiangxi 344000, P. R. China, ecitluofeng@163.com

Electronic Supplementary Information (ESI) available: [additional Figures and Table]. See DOI: 10.1039/c000000x/

1 W. C. Li, H. F. Tse, *Environ Sci Pollut Res*, 2015, **22**, 192-201.
2 S.-I. Lo, P.-C. Chen, C.-C. Huang, H.-T. Chang, *Environmental Science & Technology*, 2012, **46**, 2724-2730.
3 C. Liu, R. Bai, Q. San Ly, *Water Research*, 2008, **42**, 1511-1522.
4 O. Ozay, S. Ekici, Y. Baran, N. Aktas, N. Sahiner, *Water Research*, 2009, **43**, 4403-4411.
5 X. Tang, D. Niu, C. Bi, B. Shen, *Industrial & Engineering Chemistry Research*, 2013, **52**, 13120-13127.
6 J. De Clercq, *Int J Ind Chem*, 2012, **3**, 1-6.
7 Z. Qu, L. Yan, L. Li, J. Xu, M. Liu, Z. Li, N. Yan, *ACS Applied Materials & Interfaces*, 2014, **6**, 18026-18032.
8 K. K. Tanabe, S. M. Cohen, *Chemical Society Reviews*, 2011, **40**, 498-519.
9 a) L. J. Murray, M. Dinca, J. R. Long, *Chemical Society Reviews*, 2009, **38**, 1294-1314; b) F. Luo, C. B. Fan, M. B. Luo, X. L. Wu, Y. Zhu, S. Z. Pu, W. Y. Xu, G. C. Guo, *Angewandte Chemie International Edition*, 2014, **53**, 9298-9301.
10 L. Ma, C. Abney, W. Lin, *Chemical Society Reviews*, 2009, **38**, 1248-1256.

11 P. Horcajada, C. Serre, M. Vallet-Regí, M. Sebban, F. Taulelle, G. Férey, *Angewandte Chemie International Edition*, 2006, **45**, 5974-5978.
12 Z.-J. Lin, J. Lu, M. Hong, R. Cao, *Chemical Society Reviews*, 2014, **43**, 5867-5895.
13 M. Sohrabi, *Microchim Acta*, 2014, **181**, 435-444.
14 F. Ke, L.-G. Qiu, Y.-P. Yuan, F.-M. Peng, X. Jiang, A.-J. Xie, Y.-H. Shen, J.-F. Zhu, *Journal of Hazardous Materials*, 2011, **196**, 36-43.
15 X.-P. Zhou, Z. Xu, M. Zeller, A. D. Hunter, *Chemical Communications*, 2009, 5439-5441.
16 F. Luo, M.-S. Wang, M.-B. Luo, G.-M. Sun, Y.-M. Song, P.-X. Li, G.-C. Guo, *Chemical Communications*, 2012, **48**, 5989-5991.
17 F. Raji, M. Pakizeh, *Applied Surface Science*, 2013, **282**, 415-424.
18 J. U. K. Oubagaranadin, N. Sathyamurthy, Z. V. P. Murthy, *Journal of Hazardous Materials*, 2007, **142**, 165-174.
19 M. Tuzen, A. Sari, D. Mendil, M. Soylak, *Journal of Hazardous Materials*, 2009, **169**, 263-270.
20 H. K. Boparai, M. Joseph, D. M. O'Carroll, *Journal of Hazardous Materials*, 2011, **186**, 458-465.
21 J. Febrianto, A. N. Kosasih, J. Sunarso, Y.-H. Ju, N. Indraswati, S. Ismadji, *Journal of Hazardous Materials*, 2009, **162**, 616-645.
22 K.-K. Yee, N. Reimer, J. Liu, S.-Y. Cheng, S.-M. Yiu, J. Weber, N. Stoc, Z. Xu, *Journal of the American Chemical Society*, 2013, **135**, 7795-7798.